The Astrophysical Journal, 571:753–762, 2002 June 1

DETECTION OF THE BL LACERTAE OBJECT H1426+428 AT TeV GAMMA-RAY ENERGIES

D. Horan,[1,2] H. M. Badran,[1,3] I. H. Bond,[4] S. M. Bradbury,[4] J. H. Buckley,[5] M. J. Carson,[2] D. A. Carter-Lewis,[6] M. Catanese,[1] W. Cui,[7] S. Dunlea,[2] D. Das,[8] I. de la Calle Perez,[4] M. D'Vali,[4] D. J. Fegan,[2] S. J. Fegan,[1,9] J. P. Finley,[7] J. A. Gaidos,[7] K. Gibbs,[1] G. H. Gillanders,[11] T. A. Hall,[6,12] A. M. Hillas,[4] J. Holder,[4] M. Jordan,[5] M. Kertzman,[13] D. Kieda,[14] J. Kildea,[2] J. Knapp,[4] K. Kosack,[5] F. Krennrich,[6] M. J. Lang,[11] S. LeBohec,[6] R. Lessard,[7] J. Lloyd-Evans,[4] B. McKernan,[2] P. Moriarty,[15] D. Muller,[10] R. Ong,[16] R. Pallassini,[4] D. Petry,[6] J. Quinn,[2] N. W. Reay,[8] P. T. Reynolds,[17] H. J. Rose,[4] G. H. Sembroski,[7] R. Sidwell,[8] N. Stanton,[8] S. P. Swordy,[10] V. V. Vassiliev,[14] S. P. Wakely,[10] and T. C. Weekes[1]

Received 2001 November 29; accepted 2002 February 4

ABSTRACT

A very high energy γ-ray signal has been detected at the 5.5 σ level from H1426+428, an X-ray–selected BL Lacertae object at a redshift of 0.129. The object was monitored from 1995 to 1998 with the Whipple 10 m imaging atmospheric Cerenkov telescope as part of a general blazar survey; the results of these observations, although not statistically significant, were consistently positive. X-ray observations of H1426+428 during 1999 with the *BeppoSAX* instrument revealed that the peak of its synchrotron spectrum occurs at greater than 100 keV, leading to the prediction of observable TeV emission from this object. H1426+428 was monitored extensively at the Whipple Observatory during the 1999, 2000, and 2001 observing seasons. The strongest TeV signals were detected in 2000 and 2001. During 2001, an integral flux of $2.04 \pm 0.35 \times 10^{-11}$ cm^{-2} s^{-1} above 280 GeV was recorded from H1426+428. The detection of H1426+428 supports the idea that, as also seen in Mrk 501 and 1ES 2344+514, BL Lacertae objects with extremely high synchrotron peak frequencies produce γ-rays in the TeV range.

Subject headings: BL Lacertae objects: individual (1ES 1426+42.8) — gamma rays: observations

1. INTRODUCTION

Blazars are the main class of active galactic nuclei (AGNs) detected above 100 MeV by the EGRET experiment on the *Compton Gamma Ray Observatory* (*CGRO*) and by ground-based γ-ray observatories (Mukherjee et al. 1997; Weekes 2002). They comprise a subclass of AGN and are characterized by a highly variable nonthermal continuum, strong variable optical polarization, the lack of a UV excess (or "blue bump"), and a core-dominated radio morphology. BL Lacertae (BL Lac) objects are a subclass of blazars that are notable for their lack of prominent emission lines. The broadband double-humped spectral energy distributions (SEDs) of BL Lac objects identified in X-ray surveys differ significantly from the SEDs of those identified in radio surveys. This led to the subclassification of BL Lac objects into high-frequency peaked BL Lac objects (HBLs) and low-frequency peaked BL Lac objects (LBLs) based on the ratio of their X-ray to radio flux densities (Padovani & Giommi 1995). The first "hump," generally assumed to be the peak of the synchrotron emission (in a νF_ν representation), is in the IR-optical for LBLs and in the EUV–soft X-ray band for HBLs. BL Lac objects make up a significant fraction of the 70 blazars in the Third EGRET Catalog (Hartman et al. 1999), and most of them are classified as LBLs. It has been shown that there is not a sharp division between these two classes of objects (see, e.g., Fossati et al. 1998; Ghisellini 1999).

Recent studies with ground-based γ-ray telescopes have produced evidence for TeV γ-ray emission from seven BL Lac objects, five of which are classified as HBL and two as LBL (Weekes et al. 2002). The most prominent of these are Mrk 421, which has been detected by five ground-based imaging atmospheric Cerenkov γ-ray observatories, and Mrk 501, which has been detected by six such observatories. The emission from both of these objects can be explained by Compton-synchrotron models, although detailed modeling is still fraught with many uncertainties. Both objects are characterized by rapid variability on timescales from hours to months. In the TeV energy range, the energy spectrum of Mrk 501 and, more recently, that of Mrk 421 have been shown to exhibit absorption-like features (Krennrich et al. 1999, 2001; Aharonian et al. 1999). The temporal and spec-

[1] Fred Lawrence Whipple Observatory, Harvard-Smithsonian Center for Astrophysics, P.O. Box 97, Amado, AZ 85645; dhoran@cfa.harvard.edu.
[2] Experimental Physics Department, National University of Ireland, Belfield, Dublin 4, Ireland.
[3] Physics Department, Tanta University, Tanta, Egypt.
[4] Department of Physics, University of Leeds, Leeds, LS2 9JT Yorkshire, England, UK.
[5] Department of Physics, Washington University, St. Louis, MO 63130.
[6] Department of Physics and Astronomy, Iowa State University, Ames, IA 50011.
[7] Department of Physics, Purdue University, West Lafayette, IN 47907.
[8] Department of Physics, Kansas State University, Manhattan, KS 66506.
[9] Department of Physics, University of Arizona, Tucson, AZ 85721.
[10] Enrico Fermi Institute, University of Chicago, Chicago, IL 60637.
[11] Physics Department, National University of Ireland, Galway, Ireland.
[12] Physics and Astronomy Department, University of Arkansas at Little Rock, Little Rock, AR 72204.
[13] Department of Physics and Astronomy, DePauw University, Greencastle, IN 46135.
[14] High Energy Astrophysics Institute, University of Utah, Salt Lake City, UT 84112.
[15] School of Science, Galway-Mayo Institute of Technology, Galway, Ireland.
[16] Department of Physics, University of California, Los Angeles, CA 90095.
[17] Department of Physics, Cork Institute of Technology, Cork, Ireland.

tral properties of the other TeV BL Lac objects are less well defined.

Since 1992, the Whipple Gamma Ray collaboration, using the 10 m imaging atmospheric Cerenkov telescope on Mount Hopkins, has been searching for TeV γ-ray emission from AGNs. Initially the search was concentrated on blazars detected by EGRET at any redshift; these observations led to the detection of Mrk 421 (Punch et al. 1992) and upper limits on some 30 other blazars (Kerrick et al. 1995). More recently, the search has concentrated on nearby BL Lac objects, leading to the detection of Mrk 501 (Quinn et al. 1996) and 1ES 2344+514 (Catanese et al. 1998). Between 1995 and 1998, the survey included 24 objects (17 HBLs, 7 LBLs) ranging in redshift from 0.046 to 0.44; the results for these objects will be published shortly (Horan et al. 2000). Although none of these observations resulted in a detection, the observations of H1426+428 yielded the highest consistently positive statistical significances.

In this paper, evidence is presented for the detection of very high energy (VHE) γ-rays from H1426+428. The H1426+428 observations are divided into two categories—those taken as part of the general blazar survey between 1995 and 1998, and the subsequent concentrated observations carried out between 1999 and 2001. A preliminary energy spectrum is derived and the implications of the detection of H1426+428 at these energies are discussed.

2. H1426+428 AT OTHER WAVELENGTHS

H1426+428 was discovered in the 2–6 keV band by *HEAO 1* (Wood et al. 1984) and was classified as a BL Lac object in 1989 (Remillard et al. 1989). It has a cosmological redshift of 0.129 and is located in the constellation of Böotes ($\alpha_{J2000} = 14^h28^m32^s.7$, $\delta_{J2000} = +42°40'20''$). It is an optically faint object ($m_V = 16.9$) and is believed to be at the center of an elliptical galaxy. H1426+428 is bright in the X-ray band, with a 2–6 keV luminosity of $\sim 10^{44}$ ergs s^{-1}, which is typical of the BL Lac objects found with *HEAO 1*. Both the flux of H1426+428 in the 2–10 keV band and its spectral index above 2 keV have been found to change over time (Costamante et al. 2001).

Three recent BL Lac surveys, the Deep X-Ray Radio Blazar Survey (DXRBS; Perlman et al. 1998), the RASS Green Bank survey (RGB; Laurent-Muehleisen et al. 1999), and the Radio Emitting X-Ray Sources (REX) survey (Caccianiga et al. 1999), have shown that despite the conventional subdivision into HBLs and LBLs, BL Lac objects actually form a continuous class with respect to the peak of the synchrotron emission, which smoothly ranges between IR and soft X-ray frequencies and up to the 2–10 keV band for sources like Mrk 421. *BeppoSAX* observations of Mrk 501 (Pian et al. 1998) and 1ES 2344+514 (Giommi, Padovani, & Perlman 2000) revealed that, at least in a flaring state, the first peak of the SED can reach even higher energies at or above 100 keV.

In 1998–1999, *BeppoSAX* performed an observing campaign with the aim of finding and studying other sources as "extreme" as Mrk 501 is in its flaring state. The candidates for the *BeppoSAX* survey were selected from the *Einstein* Slew Survey and the *ROSAT* All-Sky Survey Bright Source Catalog (RASSBSC). These *BeppoSAX* observations (Costamante et al. 2000, 2001) revealed four new "extreme" HBLs, selected because they have high synchrotron peak frequencies and are therefore possible TeV emitters. These four candidates for TeV emission were 1ES 0120+340, PKS 0548−322, 1ES 1426+42.8 (i.e., H1426+428), and H2356−309.

The spectra for three of these objects (1ES 0120+340, PKS 0548−322, and H2356−309) were well fitted by a convex broken power law with a break energy, and hence the peak of the synchrotron emission, occurring at about 1.4 keV for 1ES 0120+340, 4.4 keV for PKS 0548−322, and 1.8 keV for H2356−309. In the case of H1426+428, however, no evidence for a spectral break up to 100 keV was found. Instead, its spectrum was well fitted by a single power law, with a flat spectral index of 0.92–100 keV, thus constraining the peak of the synchrotron emission to lie near or above this value. The best fit of a pure homogeneous synchrotron self-Compton (SSC) model for H1426+428 (Costamante et al. 2001) predicted detectable γ-ray emission at TeV energies. At the time of the *BeppoSAX* observation, the observed X-ray flux in the 2–10 keV band was at one of the lowest levels ever recorded from H1426+428, indicating that it was not in a flaring state (Costamante et al. 2001). This implies that, in the event of a flare, the synchrotron peak could shift to even higher values, as was observed for both Mrk 501 and 1ES 2344+514. It also indicates that highly relativistic electrons are present, which makes H1426+428 the most promising candidate for TeV emission from this survey.

3. OBSERVING TECHNIQUE

The observations reported in this paper were taken with the 10 m reflector at the Whipple Observatory on Mount Hopkins in southern Arizona (elevation 2.3 km) using the atmospheric Cerenkov imaging technique. During the course of the observations presented here, many changes were implemented on the 10 m telescope. The imaging camera (Cawley et al. 1990) was upgraded a number of times (Finley et al. 2000), the number of photomultiplier tubes (PMTs) being increased with each iteration, resulting in the current high-resolution 490 pixel camera (Finley et al. 2001). The triggering electronics were upgraded to a pattern selection trigger (Bradbury et al. 1999), and light cones were installed in front of the PMTs to increase their light collection efficiency. The unprotected, anodized, front-aluminized mirrors on the 10 m were recoated during the time span of the observations. Because of changes in PMT configuration, triggering, mirror reflectivity, and light collection efficiency, the energy response of the camera for γ-ray detection varied. Since various changes were made at the beginning of each observing season (typically between June and September), it is convenient to consider each observing season separately and to characterize it by the observed response from the assumed standard candle, the Crab Nebula. The different configurations of the camera and the resulting peak response energies are summarized in Table 1.

The Cerenkov light images from each shower are analyzed off-line using a moment analysis (Reynolds et al. 1993). The derived image parameters are used to distinguish candidate γ-rays from the large background of cosmic rays. These parameters include "length," "width," "distance" (from the optic axis), and orientation (alpha). In addition, the two highest recorded signals in individual pixels (sig1 and sig2) are noted, as well as the total light in the image ("size"). Monte Carlo simulations were used to determine the approximate limits on the parameters to be used for the

TABLE 1
CAMERA CONFIGURATIONS FROM 1995 TO 2001

Period	Number of Pixels	Spacing (deg)	FOV[a] (deg)	Light Cones	Trigger	E_{peak}[b] (GeV)
1995 Jan–1996 Dec.....	109	0.259	3.0	Yes	Majority	300
1997 Jan–1997 Jun	151	0.259	3.3	Yes	Majority	350
1997 Sep–1998 Dec	331	0.24	4.8	No	Majority	500
1999 Mar–1999 Jun.....	331	0.24	4.8	Yes	Pattern	500
1999 Sep–2000 Jul	490	0.12[c]	3.8[d]	Yes	Pattern	430
2000 Oct–2001 Jun	490	0.12[c]	3.8[d]	Yes	Pattern	390

[a] Field of view (FOV).
[b] The peak response energy (E_{peak}); this is the energy at which the collection area folded with an $E^{-2.5}$ spectrum reaches a maximum. Thus, it is the energy at which the camera is most efficient at detecting γ-rays. These values are subject to a ∼20% uncertainty. Although E_{peak} has increased somewhat over time, this does not mean that the camera is now poorer at detecting the lower energy γ-rays. In fact, the collection area of the telescope at 300 GeV in the 1999–2000 observing season was greater than the collection area at this energy in the 1995–1996 observing season.
[c] The spacing between the outer tubes is 0.°24.
[d] The outer rings of tubes were not used in this analysis, hence the field of view here is effectively 2.°6.

identification of candidate γ-ray images; these limits were then optimized on contemporaneous observations of the Crab Nebula. The results of an analysis are graphically presented as a histogram of the alpha parameter—usually referred to as an alpha plot. In such histograms, the alpha values for all the events that passed all γ-ray selection criteria, except for the alpha cut, are plotted. For a γ-ray source, an excess would be expected at low values of alpha.

Two modes of observation were used: ON/OFF and TRACKING. In ON/OFF mode, a 28 sidereal minute run is taken with the candidate γ-ray source at the center of the field of view—the ON run. The OFF run, a "control" run, is also taken for 28 sidereal minutes through the same range of azimuth and elevation, thus enabling this region of the atmosphere to be characterized in the absence of the γ-ray candidate. In the TRACKING mode, the object is continuously tracked for 28 sidereal minutes with no control run being taken.

Even in the absence of a γ-ray source, a certain percentage of events recorded will pass all of the γ-ray selection criteria. This background level of events, which depends on a number of factors, including sky brightness, elevation, and weather, needs to be established in order to calculate the statistical significance of any apparent excess of γ-rays detected. There are different methods for estimating this background, depending on which mode of observation was used.

For data taken in ON/OFF mode, the OFF scan provides an estimate of the number of γ-ray–like events that would be recorded from this range of azimuth and elevation, in the absence of the candidate γ-ray source. In this data acquisition mode, differences in night-sky brightness between the ON and OFF regions of the sky can introduce a bias when the data are analyzed. In order to reduce this bias, the standard deviations of the night-sky background in each PMT are compared for the ON and OFF runs. Gaussian noise is then added in quadrature to the signal from whichever region of the sky (ON or OFF) is darker, so as to match the standard deviations for the tube in the ON and OFF runs. This technique is known as software padding and is described in Cawley (1993).

Unlike observations taken in the ON/OFF mode, scans taken in the TRACKING mode do not have independent control data. A background estimate is essential in order to predict what number of the background events, passing all cuts, would have been detected during the scan in the absence of the candidate γ-ray source. Since most of the H1426+428 observations were taken in the TRACKING mode, two different methods of background estimation were used. Each of these methods is outlined below.

In the first method, which is the standard analysis method used for data taken in the TRACKING mode (Catanese et al. 1998), the alpha plot was characterized when there was no γ-ray source at the center of the field of view. This was done by analyzing "dark-field data," which consisted of data taken in the OFF mode and of observations of objects found not to be sources of γ-rays. A large database of these scans was analyzed, giving the shape that an alpha plot would be expected to have when no γ-rays are present.

Most γ-rays from an object at the center of the field of view will have small values of the alpha parameter. Hence, the α distribution beyond 20° can be assumed to be independent of the γ-ray source, and thus representative of the background level of γ-ray–like events in the field of view. Using the dark-field data, a ratio was calculated to scale the number of events between 20° and 65° to the number that pass the alpha cut. This ratio, the "tracking ratio" (ρ), was then used to scale the 20°–65° region of the alpha plot for the TRACKING scan, to estimate the background level of events passing all cuts. Its value and statistical uncertainty ($\Delta\rho$) are given by

$$\rho \pm \Delta\rho = \frac{N_{\rm alpha}}{N_{\rm alpha}} \pm \sqrt{\frac{N_{\rm alpha}}{N^2_{\rm control}} + \frac{N^2_{\rm alpha}}{N^3_{\rm control}}}\,, \qquad (1)$$

where N_α is defined as the number of events in the dark-field data that pass all the γ-ray selection criteria including the alpha cut, while $N_{\rm control}$ is the number of such events with alpha between 20° and 65°. The tracking ratio was calculated using the dark-field data available for each observing year over the same range of elevation angles as the source observations. In addition, the tracking ratio was checked using the OFF data on H1426+428 from ON/OFF runs

(where available); within statistics these tracking ratios were consistent with the standard tracking ratio derived from the full yearly database. To check for systematic effects associated with the determination of the global tracking ratio, the dark-field data were subdivided on the basis of the region of the sky they were from. Each of these dark-sky regions was checked individually and the tracking ratio determined and compared to the global tracking ratio. It was found that the global tracking ratio and these individual tracking ratios were consistent within statistical uncertainty.

In the alternative method for estimating the background, each H1426+428 TRACKING scan was assigned a suitable OFF scan as its background. The OFF database comprised all OFF scans taken during the observing season, including H1426+428 OFF runs. In order to establish the most suitable OFF scan for each H1426+428 TRACKING scan, each OFF run was characterized by parameters pertinent to the conditions during the scan. These consisted of the elevation, the number of PMTs switched off, and the mean night-sky background during that scan, along with the throughput factor recorded on the night of the scan and the date on which the scan was taken. The throughput factor (Holder et al. 2001) is a measure of sky clarity based on the spectrum of the total amount of light produced by background cosmic rays. The same information was assembled for each H1426+428 TRACKING scan. Then, for each H1426+428 TRACKING scan, the OFF scan whose conditions most closely matched it was deemed the most suitable background estimate and was used as the background for that H1426+428 tracking run. In cases in which there was not a suitable OFF run, the H1426+428 TRACKING run was omitted. With each H1426+428 TRACKING scan then having an associated OFF run, the data were analyzed as if they were taken in the ON/OFF mode, and hence, software padding was applied. The sky quality changes from night to night, causing variations of $\sim$10% in the raw trigger rate for data taken on the same source at the same elevation. Therefore, even after selecting OFF scans with run conditions that match those of the ON scans, it is still necessary to normalize the total number of events in the ON and the OFF. We calculate the normalizing factor from the ratio of the number of events in the 30°–90° control region of the ON and OFF alpha plots.

It was found that both methods of background estimation were consistent and indicated excesses of similar significance, thus suggesting that the γ-ray excess can be reliably determined for TRACKING scans.

4. DATABASE

For the purpose of data analysis, two different strategies were employed: (1) all of the data taken in the ON and the TRACKING modes were combined and subjected to a TRACKING analysis, and (2) all of the data taken in the ON mode, along with their corresponding OFF data, were analyzed together using the PAIRS analysis. The γ-ray selection criteria, including the alpha bound, were reoptimized each year using data from the Crab Nebula. The optimum value for the alpha bound was found empirically to increase from 10° to 15° when the smaller, high-resolution 490 pixel camera was installed in the summer of 1999.

4.1. *1995–1998 Observations*

In 1995 June–July, H1426+428 was observed for 3.5 hr in the TRACKING mode with the 109 pixel camera (spacing 0.°259, 3.°0 field of view, and standard trigger). In 1997 February–June, another 13.2 hr were used to observe H1426+428 in the TRACKING mode; the camera configuration was as before but the number of pixels was increased to 151. In 1998 April, 0.87 hr of H1426+428 data were taken; the 331 pixel camera was installed at this time with the standard trigger.

4.2. *1999 Observations*

During the 1999 observing season, a total of seven ON/OFF pairs and 51 TRACKING runs were taken with the twofold pattern selection trigger. Three TRACKING runs were excluded from further analysis based on fluctuations in the raw rate and inferior weather conditions. This left a total of 24.35 hr (7 ON runs and 48 TRACKING runs) of data available for analysis. These observations were initiated as part of the general BL Lac survey (Horan et al. 2000) with extra data being taken in 1999 because of an initial indication of a signal from H1426+428. A tracking ratio of 0.232 ± 0.005 was determined for alpha less than 10°.

4.3. *2000 Observations*

During the 2000 observing season, 33 ON/OFF pairs and 35 TRACKING runs were taken on H1426+428. Eleven ON source runs were excluded from further analysis based on fluctuations in the raw rate and inferior weather conditions, leaving a total of 26.46 hr of data available for TRACKING analysis (57 TRACKING/ON) and 13.86 hr of data in the ON/OFF mode (30 ON/OFF pairs). A tracking ratio of 0.312 ± 0.002 for alpha less than 15° was determined. H1426+428 OFF data were analyzed to ensure that this tracking ratio was consistent with the tracking ratio derived for these data.

4.4. *2001 Observations*

A total of 42.24 hr were spent on the source during 2001; this comprised 39 ON/OFF pairs and 59 TRACKING runs. After excluding data taken at low elevation and in unsatisfactory weather conditions, 38.10 hr of data remained (34 ON/OFF pairs and 53 TRACKING runs). The tracking ratio for this observing season, again for alpha less than 15°, was calculated to be 0.323 ± 0.002. As with the 2000 data, checks were performed to ensure that this ratio was appropriate for the H1426+428 data. A summary of the data taken and analyzed in the 2000 and 2001 observing seasons is given in Table 2.

5. RESULTS

5.1. *1995–1998 Observations*

The observations of H1426+428 between 1995 and 1998 were analyzed as part of a general BL Lac survey. The results are summarized in Table 3. Although not statistically significant, H1426+428 was one of only two objects, out of the 24 objects observed in this survey, to show consistently positive results.

TABLE 2

SUMMARY OF THE NUMBER OF DATA SCANS TAKEN AND ANALYZED IN 2000 AND 2001

	DATA RECORDED		DATA ANALYZED		
YEAR	TRACKING	ON	Standard	Alternative	PAIRS
2000	35 (27)	33 (30)	57	57	30
2001	59 (53)	39 (34)	87	71	34

NOTE.—The mode that the data were recorded in is given in the first two columns. The numbers in parentheses here refer to the number of usable data scans recorded. The final three columns give the number of scans analyzed in each of the three data analysis modes: standard TRACKING analysis, alternative TRACKING analysis, or PAIRS.

5.2. *1999 Observations*

A total of 24.35 hr of data were taken on H1426+428 during 1999. The net excess of $+0.9\ \sigma$ from the combined 1999 observations was not statistically significant.

5.3. *2000 Observations*

A TRACKING analysis of all the on-source data taken on H1426+428 during 2000, using the standard tracking ratio calculated for that observing season, gave a $+4.2\ \sigma$ excess, corresponding to a γ-ray rate of $0.24 \pm 0.06\ \gamma$ minute^{-1}. When these data were analyzed independently using the alternative method of background estimation, the excess was at the $+3.1\ \sigma$ level with a γ-ray rate of $0.21 \pm 0.07\ \gamma$ minute^{-1}. The alpha plot for these data is shown in Figure 1 (*left panel*) along with the alpha plot from the matched OFF data. The background shown in the figure (*dashed line*) consists of the OFF data, which were chosen to match the characteristics of the H1426+428 TRACKING data. These data are scaled to match the H1426+428 data in the 30°–90° region of the alpha plot. The net significance for the 30 ON/OFF pairs taken in 2000 was $+1.2\ \sigma$, with a γ-ray rate of $0.10 \pm 0.09\ \gamma$ minute^{-1}. The alpha plot for these data is shown in Figure 1 (*right panel*). On the night of 2000 May 30 (MJD 51694), the first TRACKING scan on H1426+428 gave a significance of $+3.0\ \sigma$, using the standard tracking ratio method of background estimation. This prompted observers to take four more TRACKING scans, which led to the detection of a signal at the $+3.7\ \sigma$ for this night. The γ-ray rate for these five scans (2.15 hr) was $0.67 \pm 0.18\ \gamma$ minute^{-1}.

5.4. *2001 Observations*

A TRACKING analysis of all of the on-source data taken on H1426+428 during 2001, using the tracking ratio calculated for this observing season, gave an excess of $+5.4\ \sigma$, corresponding to a γ-ray rate of $0.36 \pm 0.07\ \gamma$ minute^{-1}. An independent analysis of 31.13 hr of these data, using the alternative method of background estimation, resulted in a $+5.5\ \sigma$ excess with a γ-ray rate of $0.44 \pm 0.08\ \gamma$ minute^{-1}. The alpha plot for these data is shown in Figure 2 (*left panel*) along with the alpha plot from the matched OFF data. As before, these data are scaled to the H1426+428 data between alpha values of 30° and 90°.

The significance from the 34 ON/OFF pairs taken during the 2001 observing season is $+2.0\ \sigma$, with a γ-ray rate of $0.22 \pm 0.11\ \gamma$ minute^{-1}. The alpha plot for these data is shown in Figure 2 (*right panel*). A summary of the results of the observations made on H1426+428 during 2000 and 2001, using the alternative method of background estimation, is presented in Table 4.

When both the differences in exposure time and the methods of background estimation are taken into account, the results from the ON/OFF pairs and the TRACKING data taken on H1426+428 during each observing season are consistent with each other at the $2\ \sigma$ level.

5.5. *Comparison of the Gamma-Ray and X-Ray Flux from H1426+428*

The γ-ray rates for the 2000 and 2001 H1426+428 data were compared with the X-ray flux from the all-sky monitor (ASM) instrument on board the *Rossi X-Ray Timing Explorer* (*RXTE*; Levine et al. 1996). A correlation was sought between the nightly γ-ray rates and the "one-day average" X-ray data points. Only nights on which there were both X-ray and γ-ray data were considered when performing the correlation. This left 37 nights for analysis during 2000 and 39 nights during 2001.

Since γ-ray observations can only be taken on moonless nights, there are a few ($\sim$6) nights around the time of full moon each month when no observations can be made. The periods during which the γ-ray data are taken are referred to as "dark runs." Correlations between the X-ray and γ-ray rates were sought both over the entire observing season and during dark runs with more than two nights on which both X-ray and γ-ray data were taken. No evidence for significant nightly correlation was found for either observing season. The X-ray and γ-ray rate curves are shown in

TABLE 3

SUMMARY OF THE OBSERVATIONS AND RESULTS FOR H1426+428 BETWEEN 1995 AND 1999

Period	Exposure (hr)	Total σ	Maximum σ Month[a]	Maximum σ Night[b]	Flux[c] (cm^{-2} s^{-1})
1995 Jun–1995 Jul	3.48	2.1	2.1	2.1	$<0.2 \times 10^{-11}$
1997 Feb–1997 Jun.....	13.16	1.7	2.2	1.6	$<0.1 \times 10^{-11}$
1998 Apr	0.87	1.7	1.7	2.0	$<6.7 \times 10^{-11}$
1999 Mar–1999 Jun.....	24.35	0.9	1.6	2.1	$<6.7 \times 10^{-11}$

[a] The maximum statistical significance of the signal recorded from H1426+428 when the data are grouped by the month during which they were recorded.

[b] The maximum statistical significance of the signal recorded from H1426+428 when the data are grouped by the night on which they were recorded.

[c] The integral fluxes are quoted at the peak response energy for the observation period, as given in Table 1.

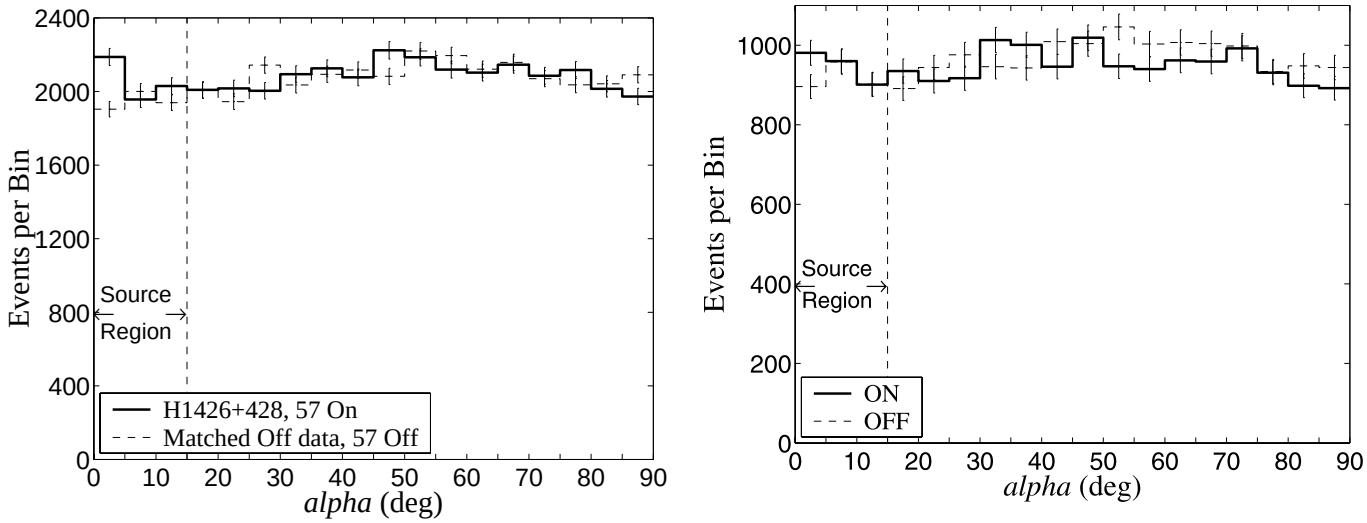

FIG. 1.—*Left*: Alpha plot for 26.49 hr of the data taken on H1426+428 during 2000. The total significance for these 57 scans is +3.1 σ when analyzed using the alternative method for estimating the background. The matched OFF data used to estimate the background level are also shown (*dashed line*). These are normalized to the H1426+428 data between alpha values of 30° and 90°. *Right*: Alpha plot for the 30 ON/OFF pairs taken in 2000. The net significance for these data is +1.2 σ.

Figure 3. The rates plotted here are the average monthly rates for the 2000 and 2001 data. The γ-ray rates shown were calculated using the alternative method of background estimation. There is some evidence for an anticorrelation between these average monthly rates, especially in the 2001 data.

6. SPECTRAL CHARACTERISTICS OF H1426+428

The TeV flux from H1426+428 is weak and near the threshold of sensitivity of the 10 m γ-ray telescope. The photon flux is so small that it is impractical to apply standard spectral analysis techniques, for example, Mohanty et al. (1998), to these data. In fact, only the differential flux from the source for the energy at which the telescope is most efficient at detecting γ-rays can be evaluated with reasonable accuracy. Such a flux estimate accounts mostly for the photons with energies corresponding to the peak in the differential detection rate of the telescope. This energy, E_p, depends on the spectral index of the source in question. For observations of H1426+428 with the Whipple telescope in 2001, E_p was found to be between 280 and 360 GeV. The rate of change of the number of excess events, presumably photons from the source, with the total amount of light in the Cerenkov image, the size, is directly related to the spectral index of the source. This relationship is established using Monte Carlo simulations; the spectral index of the source in the vicinity of E_p is then evaluated. This in turn allows estimates

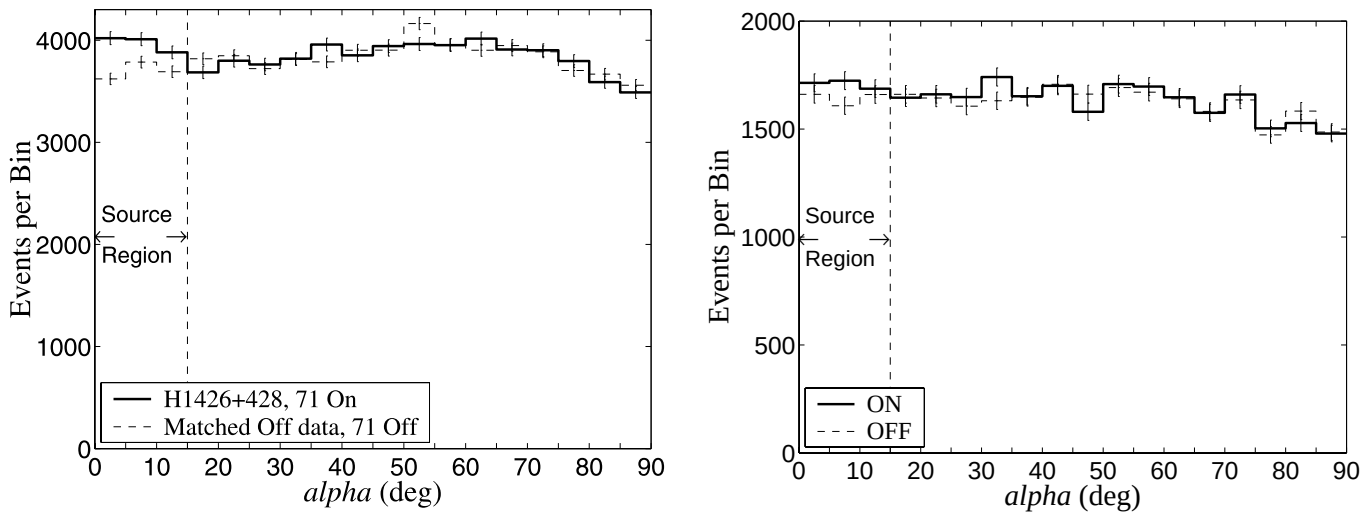

FIG. 2.—*Left*: Alpha plot for 31.13 hr of the data taken on H1426+428 during 2001. The total significance for these 71 scans, when analyzed using the alternative method of background estimation, is +5.5 σ. The matched OFF data used to estimate the background level are also shown (*dashed line*). These are normalized to the H1426+428 data between alpha values of 30° and 90°. *Right*: Alpha plot for the 15.53 hr of data taken in the ON/OFF mode on H1426+428 during 2001. The total significance for these 34 ON/OFF pairs is +2.0 σ.

TABLE 4
SUMMARY OF THE RESULTS OF H1426+428 OBSERVATIONS DURING 2000 AND 2001

Period	Exposure (hr)	Total σ	Maximum σ Month[a]
2000 Feb–2000 Jun.....	26.37	3.1	3.4
2001 Jan–2001 Jun	31.12	5.5	5.0

[a] The maximum statistical significance of the signal recorded from H1426+428 when the data are grouped by the month during which they were recorded.

of E_p for this spectral index and the differential and integral fluxes to be improved by reducing the uncertainty due to the unknown spectral index.

Figure 4 shows the excess events detected from the direction of H1426+428 as a function of integrated Cerenkov light in the shower image. For comparison, this plot also shows the excess events detected from the Crab Nebula after a 4.1 hr exposure, which was chosen to produce a similar maximal excess of $\sim 10^3$ events, as was found during the 32.5 hr of observation of H1426+428 during 2001. The lowest size cut of 366 digital counts is the result of signal-to-noise optimization of the H1426+428 data, producing an overall significance close to $+6\ \sigma$. The highest size cut, 840 digital counts, is limited by the rapidly declining significance to the level of $+3.5\ \sigma$. To a first approximation, the dependence of the excess events on the logarithm of the size cut applied is a linear function whose slope is monotonically related to the spectral index of the source. This plot indicates that the H1426+428 spectrum is softer than the well-studied spectrum of the Crab Nebula.

Monte Carlo simulations were used to relate the observed parameters of linear fits to the data in Figure 4, the spectral characteristics of H1426+428, and the Crab Nebula. The statistical correlation of the errors shown in this integral plot of excess events has been taken into account to derive optimal estimates of the spectral indices, differential and integral fluxes, and their errors. A summary of the results is given in Table 5. For the Crab Nebula, a spectral index of 2.75 with an uncertainty of 6% (1 σ) was derived. The peak of the differential detection rate of the Whipple telescope from a source with such a spectral index has been found to be around 360 GeV (2001 observing season). Based on the small Crab Nebula data set, the spectral index as well as the differential and integral fluxes have been derived, and are found to be consistent, at the 2 σ level, with our previous observations (Hillas et al. 1998). Analysis of the H1426+428 data set indicates a substantially steeper spectral index of 3.55 with a 13% relative error. For this spectral index and the 366 digital counts size cut applied in the data

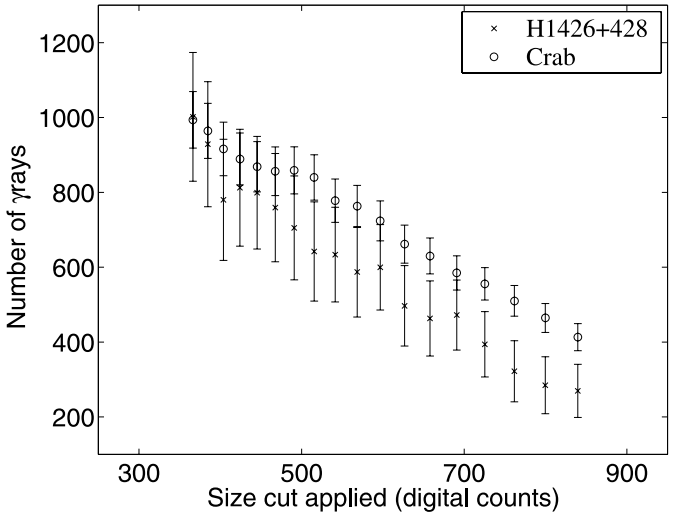

FIG. 4.—Integral excess events observed by the Whipple telescope from the directions of H1426+428 (*crosses*) and the Crab Nebula (*open circles*) during 2001 as a function of integrated Cerenkov light in the shower image. Exposure on the Crab Nebula was adjusted to match the total excess of H1426+428 at the lowest size cut applied, 366 digital counts. One photoelectron corresponds to ~3.6 digital counts.

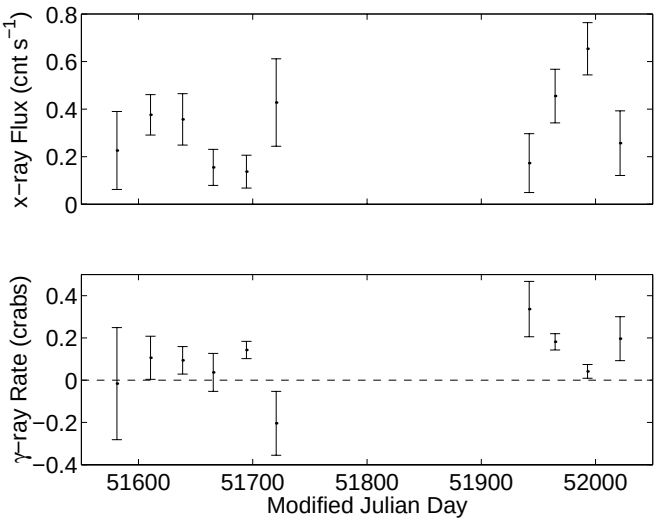

FIG. 3.—*Top*: The mean X-ray rate for H1426+428 for each month during 2000 and 2001 from the ASM on *RXTE*. The data are only plotted for months during which γ-ray data were also taken. *Bottom*: The mean γ-ray rate from H1426+428 for each month calculated using the alternative method for background estimation. This rate is plotted in units of the γ-ray rate from the Crab for that year. The detected Crab rate was 2.45 γ minute^{-1} during 2000 and 3.36 γ minute^{-1} during 2001.

TABLE 5
RESULTS OF THE SPECTRAL ANALYSIS OF H1426+428 AND CRAB NEBULA DATA SETS

Parameter	Crab	H1426 + 428	H1426 + 428
χ^2	20.60	22.72	22.72
Degrees of freedom	16	16	16
T (s)	14.7×10^3	117.3×10^3	117.3×10^3
α	2.75	3.55	3.55
E_p (GeV)	360	280	390
F_p (cm^{-2} s^{-1})	1.10×10^{-10}	2.04×10^{-11}	8.76×10^{-12}
dF_p (cm^{-2} s^{-1} TeV^{-1})	5.34×10^{-10}	1.86×10^{-10}	5.73×10^{-11}
νF_ν (erg cm^{-2} s^{-1})	1.11×10^{-10}	2.33×10^{-11}	1.39×10^{-11}
$\Delta\alpha/\alpha$	0.06	0.13	0.13
$\Delta F_p/F_p$	0.07	0.17	0.23
$\Delta dF_p/dF_p$	0.11	0.25	0.17

NOTE—α is the spectral index of the differential flux. E_p denotes the energy at which the differential detection rate of photons from a given source, with given observation and data analysis conditions, peaks. F_p and dF_p are estimates of the integral and differential fluxes at E_p.

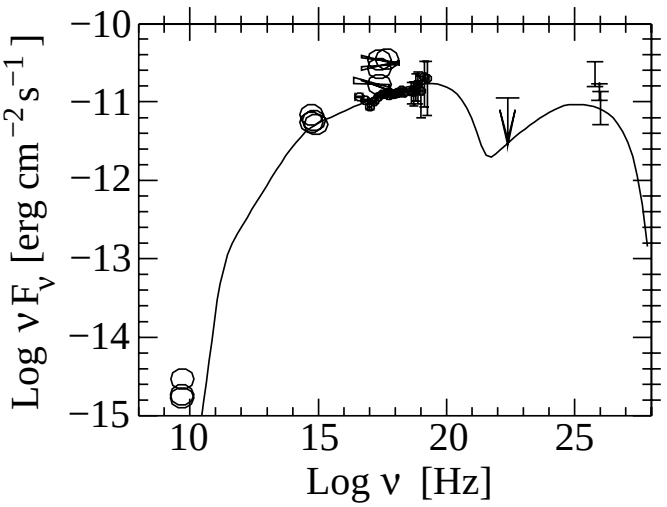

FIG. 5.—SED of H1426+428 from Costamante et al. 2001, along with the observational results obtained with the Whipple telescope. The 280 GeV ($\log \nu = 25.83$) and 390 GeV ($\log \nu = 25.97$) data points, derived from the 2001 data set, suggest a differential spectral index of the energy flux equal to −3.55. The 430 GeV ($\log \nu = 25.99$) point is a detection by the Whipple telescope during 2000. This result is subject to a large uncertainty associated with the weak detection and unknown spectral properties of the source. The EGRET upper limit above 100 MeV of 0.7×10^{-7} cm^{-2} s^{-1} is also shown, as are the fluxes from various X-ray, optical, and radio experiments, all taken from Costamante et al. 2001.

analysis, the differential photon detection rate peaks at ~280 GeV. Table 5 shows estimates of the fluxes at 390 GeV, assuming the same spectral index. This energy was chosen by increasing the size cut until the signal-to-noise ratio decreased to ~4.5 σ; below this value the signal was not considered strong enough for reliable calculation of the H1426+428 flux.

The observed energy fluxes of H1426+428 at 280 and 390 GeV are shown in Figure 5, together with the predicted SED for this source suggested by Costamante et al. (2001). This figure also shows the tentative detection (+3.1 σ) made by the Whipple 10 m telescope during 2000. Operating at a substantially higher peak response energy at that time, the Whipple telescope observed this source at $E_{\rm peak} \sim 430$ GeV. Based on these data, an estimate of the energy flux of $0.86 \pm 0.33 \times 10^{-11}$ erg cm^{-2} s^{-1} has been derived. Because of the very weak signal, however, we have not attempted to find the spectral index of H1426+428 for this data set. As a result, the indicated error is only statistical, and it does not include errors associated with the unknown spectral properties of the source. The 430 GeV peak energy itself is subject to a similar uncertainty.

7. DISCUSSION

Observations of H1426+428 with the Whipple 10 m telescope since 1995 have returned consistently positive excesses, although the statistical significance has not always been high. H1426+428 was on the very short list of predicted TeV emitters published by the *BeppoSAX* collaboration (Costamante et al. 2001) and was also singled out as the most probable TeV emitter among these because of the high frequency of its synchrotron peak. It was observed as part of a BL Lac survey at the Whipple Observatory between 1995 and 1998, and was singled out for more extensive observations between 1999 and 2001. The strongest evidence for VHE emission was recorded during the 2000 and 2001 observing seasons, with signals at the 3.1 and 5.5 σ levels, respectively, being detected. Although it is difficult to combine results from different configurations of the camera, the combined significance of the results from 2000 and 2001 is clearly equivalent to a greater than 5 σ detection, the usual level required to establish the existence of a new TeV source.

There have been two occasions (in 1999 and 2000) when there was marginal evidence for a transient signal from H1426+428. In 1999, after 2.3 hr of observations (over two nights), a signal at the +3.1 σ level was recorded, while in 2000, a signal at the +3.7 σ level was recorded after 2.2 hr of observations (on a single night).

After 18.1 hr of observations on H1426+428, the CAT collaboration reported a 3 σ upper limit of 3.54×10^{-11} cm^{-2} s^{-1} at an energy threshold of 250 GeV (Piron 2000). These observations were carried out at the beginning of 1999 February in response to an announcement from the *BeppoSAX* and the RXTE/ASM teams, which revealed H1426+428 to be transitioning to a high state.

If independently verified, the observations reported here represent an important addition to the catalog of TeV-emitting BL Lac objects (Table 6). That the source was predicted to be a TeV γ-ray source based on its X-ray spectrum is important in that it signifies the maturity of the observational techniques and the theoretical understanding of BL Lac objects. It reinforces the symbiosis between observations at X-ray wavelengths, particularly in hard X-rays, and those at TeV energies, particularly those with good sensitivity below energies of 1 TeV. The existence of a population of sources whose most prominent emission is at energies of 10–100 keV and 300–1000 GeV points to a fruitful overlap between the next generation of ground-based atmospheric Cerenkov telescopes (Weekes et al. 2002) and the future hard X-ray experiment, EXIST (Grindlay et al. 2000). It is also remarkable in that this source, like Mrk 501 and 1E2344+514, is not included in the Third EGRET Catalog, supporting the interpretation of Ghisellini (1999) that in blazars sufficiently powerful to be detected readily by EGRET, the spectrum will terminate at lower energies and not extend to the TeV domain.

Although the properties of H1426+428 reported here are scanty in comparison with the other, better studied TeV BL Lac objects, they agree in principle with the characteristics now well established for Mrk 421 and Mrk 501 (and to a lesser extent, 1ES 2344+514). Although the flux from H1426+428 is low, there is some evidence for time variability. There is no evidence for a correlation of X-ray and TeV γ-ray fluxes (unlike Mrk 501), but the sensitivity of observations to date is limited, and even in the stronger sources this correlation has been shown to be complicated.

Ghisellini (1999) has proposed that there is a continuous sequence of BL Lac objects with the peak of the synchrotron spectrum increasing as the luminosity decreases. H1426+428 is another example of an "extreme" BL Lac characterized by a synchrotron spectrum that may peak near 100 keV and a relatively weak luminosity. These objects are the best candidates for TeV emission based on Compton-synchrotron models of BL Lac jets. However, the observed variations in sources such as Mrk 501 cannot be accounted for by simple one-zone homogeneous self-Comp-

TABLE 6
EXTRAGALACTIC TeV SOURCES (CATANESE & WEEKES 1999)

Source	Type	z	Discovery	Group	EGRET
Mrk 421	HBL	0.031	1992	Whipple[a]	yes
Mrk 501	HBL	0.034	1995	Whipple[b]	yes
1ES 2344+514.....	HBL	0.044	1997	Whipple[c]	no
1ES 1959+650.....	HBL	0.048	1999	Telescope Array[d]	no
PKS 2155-304	HBL	0.116	1999	Durham[e]	yes
H1426+428.....	HBL	0.129	2001	Whipple [f]	no
3C 66A.....	LBL	0.444	1998	Crimea[g]	yes
BL Lacertae	LBL	0.069	2001	Crimea[h]	yes

[a] Punch et al. 1992.
[b] Quinn et al. 1996.
[c] Catanese et al. 1998.
[d] Nishiyama et al. 2000.
[e] Chadwick et al. 1999.
[f] Horan et al. 2000, 2001a, 2001b.
[g] Neshpor et al. 1998.
[h] Neshpor et al. 2001.

ton models and may require another source of optical target photons. It will require the detection of a greater population of sources like H1426+428 to test these models fully. It has been noted (Ghisellini 1998) that these TeV-emitting BL Lac objects are also characterized by a relatively strong radio luminosity, and that the radio luminosity may be a measure of the density of additional seed photons at infrared–optical wavelengths needed to explain the TeV emission.

This is the most distant of the TeV detected BL Lac objects classified as HBL, and hence it has promising implications for the detection of more BL Lac objects at $z > 0.1$. Stronger detections of such sources, which allow an accurate measure of the TeV energy spectrum, may place significant limits on the density of the intergalactic background light. The steep spectrum derived here is consistent with many models of intergalactic absorption but could also be intrinsic to the source.

Interpretation of the theoretical prediction of the intrinsic spectrum of H1426+428 and the observational results reported in this paper are complicated by the possible strong attenuation of the high-energy photons by the diffuse intergalactic infrared background. The appearance of such a cutoff in the spectra of TeV extragalactic sources was suggested in one of the pioneering works on TeV γ-ray absorption, by Stecker, de Jager, & Salamon (1992), for the quasar 3C 279 ($z = 0.54$). A later paper (V. V. Vassiliev et al. 2002, in preparation) will discuss this subject in detail in relation to H1426+428; here we note only that at 280 GeV, the attenuation optical depth can be anywhere between z of 0.1 and 1.0, depending on the extreme upper and lower limits known for the density of the extragalactic background light. Because of this potentially large absorption effect, it is possible, for example, that the intrinsic spectral index of this source is softened by ~1.75 to produce the observed value of 3.55, if the intrinsic properties of H1426+428 are similar to those of Mrk 501 (Vassiliev et al. 2001). It remains certain, however, that being the most distant HBL detected at sub-TeV energies, the observed spectral properties of H1426+428 and the understanding of its intrinsic characteristics from multiwavelength observations will provide the most constraining data for extragalactic background light studies.

The authors would like to thank Kevin Harris, Joe Melnick, Emmet Roach, and all the staff at the Whipple Observatory for their support. We also thank the referee for many constructive and useful suggestions. This research was supported in part by the US Department of Energy, PPARC, and Enterprise Ireland.

APPENDIX A

TABLE A1

DATA LOG FOR THE 2000 AND 2001 H1426+428 OBSERVATIONS

MJD Start Time [Mode]				
51577.48031 [p]	51672.28898 [t]	51941.43213 [t]	51970.44161 [t]	51994.37299 [p]
51577.52101 [t]	51687.17778 [t]	51941.52991 [t]	51970.49679 [t]	51994.41703 [p]
51578.49144 [p]	51687.19735 [t]	51942.43760 [t]	51970.51712 [t]	51995.49070 [p]
51579.47485 [p]	51687.21689 [t]	51944.49363 [t]	51971.43684 [t]	51996.43112 [t]
51579.51770 [t]	51687.23145 [t]	51957.37136 [p]	51971.45942 [t]	51996.47550 [t]
51581.48048 [p]	51688.17238 [p]	51957.39284 [t]	51972.44811 [t]	51997.35435 [p]
51585.50929 [t]	51689.17450 [p]	51959.39676 [p]	51972.47175 [t]	51997.44241 [t]
51586.50519 [t]	51690.17385 [p]	51959.42716 [t]	51986.36833 [p]	51997.46204 [t]
51604.43009 [t]	51692.20786 [t]	51959.44517 [t]	51988.33540 [p]	51998.40471 [t]
51605.40456 [p]	51692.24942 [p]	51960.37838 [p]	51988.35239 [t]	51998.44546 [p]
51607.43234 [p]	51693.16773 [p]	51960.40149 [t]	51989.38498 [t]	51999.41745 [p]
51617.42927 [p]	51694.17954 [t]	51960.44430 [p]	51989.43090 [p]	51999.45334 [p]
51632.35804 [t]	51694.19409 [t]	51960.46341 [t]	51990.39131 [t]	52000.40087 [t]
51632.37754 [t]	51694.22455 [p]	51960.48046 [t]	51990.43151 [p]	52000.44380 [p]
51635.31200 [t]	51694.26542 [p]	51960.50067 [t]	51990.46683 [t]	52020.23130 [p]
51635.33273 [t]	51694.30629 [p]	51961.37826 [p]	51991.40168 [p]	52022.57165 [p]
51636.35315 [p]	51695.17682 [p]	51961.39750 [t]	51991.41978 [t]	52046.22484 [p]
51637.30195 [p]	51695.21768 [p]	51961.43929 [p]	51991.43755 [t]	52047.31743 [t]
51638.35877 [p]	51695.25854 [p]	51961.47573 [t]	51991.46142 [t]	52049.27725 [t]
51641.30764 [p]	51696.26489 [t]	51961.49286 [t]	51991.47977 [t]	52050.19936 [p]
51642.36119 [t]	51698.17804 [t]	51962.39036 [p]	51992.38284 [p]	52050.23721 [p]
51642.37579 [t]	51699.17421 [p]	51962.40577 [t]	51992.43252 [p]	52051.19595 [p]
51644.36277 [t]	51700.23519 [p]	51962.43053 [p]	51992.47643 [t]	52051.26034 [p]
51645.36182 [p]	51701.25211 [p]	51963.38181 [t]	52275.18178 [p]	52053.23280 [p]
51659.25434 [p]	51702.28313 [t]	51963.42351 [t]	52275.18443 [t]	52055.26242 [p]
51659.29540 [t]	51702.30271 [t]	51963.46618 [t]	52275.18320 [t]	52056.30267 [p]
51667.28374 [p]	51720.18600 [t]	51963.48589 [t]	52275.18199 [t]	52071.24343 [t]
51669.26859 [p]	51721.18547 [p]	51965.45873 [t]	52275.18201 [t]	52072.21843 [t]
51672.26933 [t]	51940.53791 [t]	51967.46276 [t]	52275.18178 [t]	

NOTE.—The number in brackets after the MJD gives the mode in which the data were taken: p: PAIRS, t: TRACKING.

REFERENCES

Aharonian, F., et al. 1999, A&A, 349, 11
Bradbury, S. M., Burdett, A. M., D'Vali, M., Ogden, P. A., & Rose, H. J. 1999, AIP Conf. Proc. 516, Proc. 26th International Cosmic-Ray Conference, ed. B. L. Dingus, D. B. Kieda, & M. H. Salamon (Melville: AIP), 263
Caccianiga, A., Maccacaro, T., Wolter, A., della Ceca, R., & Gioia, I. M. 1999, ApJ, 513, 51
Catanese, M., & Weekes, T. C. 1999, PASP, 111, 1193
Catanese, M., et al. 1998, ApJ, 501, 616
Cawley, M. F. 1993, in Towards a Major Cerenkov Detector II, ed. R. C. Lamb (Ames: Iowa State University), 176
Cawley, M. F., Fegan, D. J., Harris, K., Kwok, P. W., & Hillas, A. M. 1990, Exp. Astron., 1, 173
Chadwick, P. M., et al. 1999, ApJ, 513, 161
Costamante, L., et al. 2000, Mem. Soc. Astron. Italia, 72, 153
———. 2001, A&A, 371, 512
Finley, J. P., et al. 2000, AIP Conf. Proc. 515, GeV-TeV Gamma Ray Astrophysics Workshop: Toward a Major Atmospheric Cerenkov Detector VI, ed. B. L. Dingus, D. B. Kieda, & M. H. Salamon (Melville: AIP), 301
———. 2001, Proc. 27th Int. Cosmic-Ray Conf. (Hamburg), 2827
Fossati, G., et al. 1998, MNRAS, 299, 433
Ghisellini, G. 1998, MNRAS, 301, 451
———. 1999, Astropart. Phys., 11, 11
Giommi, P., Padovani, P., & Perlman, E. 2000, MNRAS, 317, 743
Grindlay, J., et al. 2000, AIP Conf. Proc. 510, The Fifth Compton Symposium, ed. M. L. McConnell & J. M. Ryan (Melville: AIP), 784
Hartman, R. C., et al. 1999, ApJS, 123, 79
Hillas, A. M., et al. 1998, ApJ, 503, 744
Holder, J., et al. 2001, Proc. 27th Int. Cosmic-Ray Conf. (Hamburg), 2613
Horan, D., et al. 2000, AAS, HEAD Meeting, 32, 05.03
———. 2001a, AIP Conf. Proc. 578, Gamma-Ray Astrophysics 2001, ed. S. Ritz, N. Gehrels, & C. R. Shrader (Melville: AIP), 324
———. 2001b, Proc. 27th Int. Cosmic-Ray Conf. (Hamburg), 2622
Kerrick, A. D., et al. 1995, ApJ, 452, 588
Krennrich, F., et al. 1999, ApJ, 511, 149
———. 2001, ApJ, 560, L45
Laurent-Muehleisen, S. A., Kollgaard, R. I., Feigelson, E. D., Brinkmann, W., & Siebert, J. 1999, ApJ, 525, 127
Levine, A. M., et al. 1996, ApJ, 469, L33
Mohanty, G., et al. 1998, Astropart. Phys., 9, 15
Mukherjee, R., et al. 1997, ApJ, 490, 116
Neshpor, Y. I., Chalenko, N. N., Stepanian, A. A., Kalekin, O. R., Jogolev, N. A., Fomin, V. P., & Shitov, V. G. 2001, Astron. Rep., 45, 249
Neshpor, Y. I., Stepanyan, A. A., Kalekin, O. P., Fomin, V. P., Chalenko, N. N., & Shitov, V. G. 1998, Astron. Lett., 24, 134
Nishiyama, T., et al. 2000, AIP Conf. Proc. 516, Proc. 26th International Cosmic Ray Conference, ed. B. L. Dingus, D. B. Kieda, & M. H. Salamon (Melville: AIP), 370
Padovani, P., & Giommi, P. 1995, ApJ, 444, 567
Perlman, E. S., Padovani, P., Giommi, P., Sambruna, R., Jones, L. R., Tzioumis, A., & Reynolds, J. 1998, AJ, 115, 1253
Pian, E., et al. 1998, ApJ, 492, L17
Piron, F. 2000, Ph.D. thesis, Université de Paris-Sud U. F. R. Scientifique d'Orsay
Punch, M., et al. 1992, Nature, 358, 477
Quinn, J., et al. 1996, ApJ, 456, L83
Remillard, R. A., Tuohy, I. R., Brissenden, R. J. V., Buckley, D. A. H., Schwartz, D. A., Feigelson, E. D., & Tapia, S. 1989, ApJ, 345, 140
Reynolds, P. T., et al. 1993, ApJ, 404, 206
Stecker, F. W., de Jager, O. C., & Salamon, M. H. 1992, ApJ, 390, L49
Vassiliev, V. V., et al. 2001, Proc. 27th Int. Cosmic-Ray Conf. (Hamburg), 2725
Weekes, T. C. 2001, AIP Conf. Proc. 578, Gamma-Ray Astrophysics 2001, ed. S. Ritz, N. Gehrels, & C. R. Shrader (Melville: AIP), 324
Weekes, T. C., et al. 2002, Astropart. Phys., in press
Wood, K. S., et al. 1984, ApJS, 56, 507